Heteroleptic Copper(I) Complexes Prepared from Mono-and Tetra-phenylbenzene-substituted Phenanthroline Ligands

Brigino Ralahy, Uwe Hahn, Emeric Wasielewski, Jean-François Nierengarten

Heteroleptic Copper(I) Complexes Prepared from Mono- and Tetra-phenylbenzene-substituted Phenanthroline Ligands

Brigino Ralahy,[a] Uwe Hahn,[a] Emeric Wasielewski,[b] and Jean-François Nierengarten*[a]

Dedicated to Prof. Michael J. Chetcuti on the occasion of his 65th birthday

[a] B. Ralahy, Dr. U. Hahn, Dr. J.-F. Nierengarten
Laboratoire de Chimie des Matériaux Moléculaires
Université de Strasbourg et CNRS (UMR 7402 LIMA), Ecole Européenne de Chimie, Polymères et Matériaux
25 rue Becquerel, 67087 Strasbourg Cedex 2, France
E-mail: nierengarten@unistra.fr
[b] Dr. E. Wasielewski
Plateforme RMN Cronenbourg
Université de Strasbourg et CNRS (UMR 7402 LIMA), Ecole Européenne de Chimie, Polymères et Matériaux
25 rue Becquerel, 67087 Strasbourg Cedex 2, France

Supporting information for this article is given via a link at the end of the document.

Abstract: Phenanthroline ligands bearing two biphenyl (**L1**) or two tetraarylbenzene (**L2**) substituents have been synthetized and used to prepare bis-phenanthroline copper(I) complexes. Steric constrains are limited in the case of the biphenyl-substituted ligand and $[Cu(\mathbf{L1})_2](BF_4)$ has been obtained by reaction of **L1** with $[Cu(CH_3CN)_4](BF_4)$. In contrast, the tetraarylbenzene substituents of **L2** are large enough to totally prevent the formation of the corresponding homoleptic bis-phenanthroline copper(I) complex. Both **L1** and **L2** have been also combined with 2,9-dimethyl-1,10-phenanthroline (dmp) to prepare the corresponding heteroleptic bis-phenanthroline copper(I) complexes. All the copper(I) complexes obtained from **L1** and **L2** revealed dynamic conformational exchange between several atropisomers. Detailed NMR studies and Density Functional Theory (DFT) calculations have been carried out to assess their conformations in solution.

Introduction

The coordination of diimine aromatic ligands with copper(I) has been widely used for the construction of fascinating metallo-supramolecular nanostructures.[1] Classical examples include helicates,[2] cages[3] and molecular grids.[4] In these particular cases, the kinetic instability of the copper(I) complexes leading to ligand dissociation in solution is a clear advantage. The dynamic character allows actually for correction of possible errors during the self-assembly process and the equilibrium is therefore totally driven towards the most stable product.[1] On the other hand, this kinetic instability means also that the coordination of different ligands around the same copper(I) cation is particularly difficult to control.[5] The pioneering work of Sauvage has shown that the heteroleptic coordination of copper(I) can be favored by combining a macrocyclic chelating ligand with an acyclic one.[6] The assembly of two macrocyclic ligands around a tetracoordinated copper(I) cation is not possible and formation of a homoleptic complex from the acyclic ligand would generate a frustrated metal-ligand assembly in which all the metal-binding sites of the macrocycle are not utilized. As a result, the dynamic coordination equilibrium is totally displaced in favor of the heteroleptic complex. Another very efficient strategy to control the coordination of two different ligands around a copper(I) cation has been developed by Schmittel and co-workers.[7] In this case, one of the two chelating ligands is decorated with large substituents preventing the formation of a stable homoleptic copper(I) complex. This construction principle is shown in Figure 1 for the heteroleptic complex resulting from the combination of 2,9-dimethyl-1,10-phenanthroline (dmp) and 2,9-dimesityl-1,10-phenanthroline (dMesp).

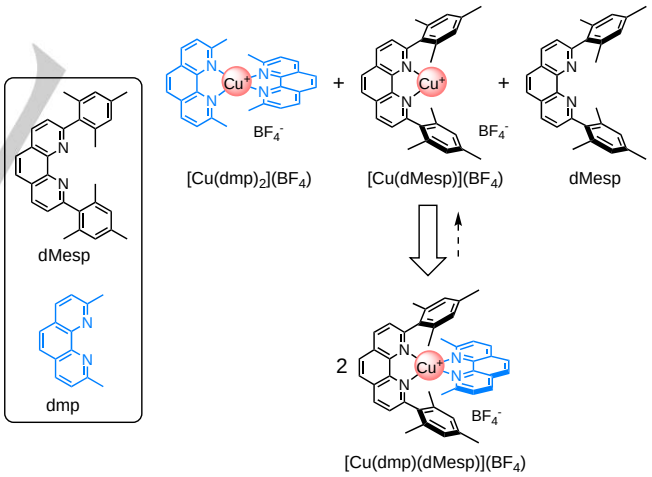

Figure 1. Control of the thermodynamic complexation scenario based on steric constraints developed by Schmittel and co-workers. The formation of heteroleptic complex $[Cu(dmp)(dMesp)]^+$ is favoured because all the ligands are used to generate coordinatively saturated copper(I) complexes. Formation of $[Cu(dmp)_2]^+$ is disfavoured because it would generate a frustrated metal-ligand assembly for ligand dMesp.

Steric constraints resulting from the bulky mesityl substituents of dMesp prevent the formation of the homoleptic complex $[Cu(dMesp)_2]^+$. Consequently, formation of the homoleptic complex from dmp would generate a mixture of free ligand (dMesp) and partially coordinated $[Cu(dMesp)]^+$. According to the maximum occupancy principle,[8] such a situation is not favorable from a thermodynamic point of view. In contrast,

formation of the heteroleptic complex $[Cu(dmp)(dMesp)]^+$ generates only coordinatively saturated copper(I) cations with all the ligands incorporated in complexes. In this case, the perfect match between the number of ligands and the coordination number of the copper(I) cations fulfils the maximum occupancy principle. As a result, formation of the heteroleptic complex is by far more favorable. As part of this research, we became interested in evaluating the potential of new diaryl-1,10-phenanthroline ligands for the formation of stable heteroleptic copper(I) complexes. In the design of these ligands, the two aryl subunits have been only substituted in one *ortho* position. As a result, their relative orientation is either *Syn* or *Anti* thus leading to an unprecedented isomerism in the resulting copper(I) complexes. Interestingly, the *Anti* isomers have been exclusively observed in the solid state. Detailed dynamic NMR studies have been carried out to assess the conformations present in solution. These experimental results have been analyzed with the help of Density Functional Theory (DFT) calculations.

Results and Discussion

Preparation of the ligands. The preparation of ligands **L1** and **L2** is depicted in Scheme 1. Treatment of 2-bromo-1,1'-biphenyl (**1**) with *n*-butyllithium (*n*BuLi) followed by reaction of the resulting [1,1'-biphenyl]-2-yl lithium with 1,10-phenanthroline under the conditions developed by Sauvage[9] gave **2** in 72% yield. The second biphenyl unit was then introduced by reaction of [1,1'-biphenyl]-2-yl lithium with **2** followed by hydrolysis and rearomatization with MnO_2. Ligand **L1** was thus obtained in 82% yield.

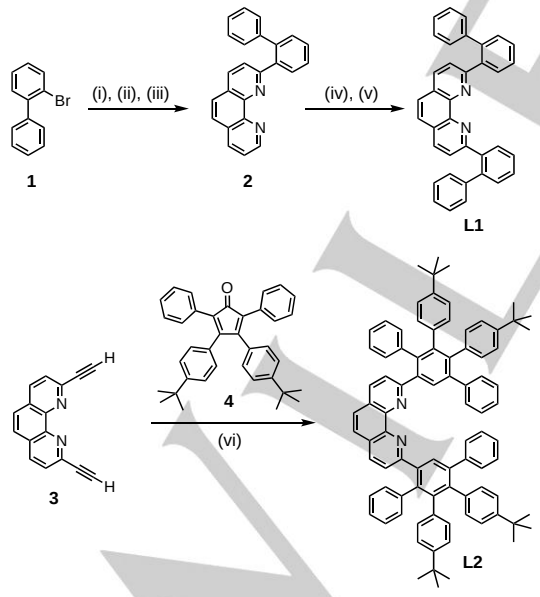

Scheme 1. Preparation of ligands **L1** and **L2**. *Reagents and conditions*: (i) *n*BuLi, Et_2O, 0°C to rt; (ii) 1,10-phenanthroline, 0°C then H_2O; (iii) MnO_2, CH_2Cl_2 (72%); (iv) [1,1'-biphenyl]-2-yl lithium, Et_2O, 0°C to rt then H_2O; (v) MnO_2, CH_2Cl_2 (82%); (vi) *o*-xylene, Δ (71%).

The preparation of ligand **L2** relies on the Diels-Alder reaction of a terminal alkyne with a tetraphenylcyclopentadienone derivative.[10] Phenanthroline building block **3** was prepared according to a previously reported procedure.[11] Compound **4** with its two *t*-butyl solubilizing groups was selected as the cyclopentadienone reagent.[12] Treatment of **3** with a slight excess of **4** (2.05 equiv.) in *o*-xylene under reflux for 12 h afforded **L2** in 71% yield.

Ligands **L1** and **L2** were fully characterized by NMR and IR spectroscopies as well as by mass spectrometry. In both cases, there are two possible relative orientations for the *o*-substituents of the phenyl moieties attached to the phenanthroline core leading to a *Syn*/*Anti* isomerism (Figure 2). ^{1}H NMR spectra were recorded at low temperature but under our experimental conditions rapid exchange between the two conformers remained faster than the NMR timescale even at 203 K (see the Supplementary Information). Computational studies were performed at the B3LYP/6-31G* level in order to further understand the conformation of **L1** and **L2**. The calculated *Syn* anti *Anti* atropisomers of both **L1** and **L2** are shown in Figure 2.

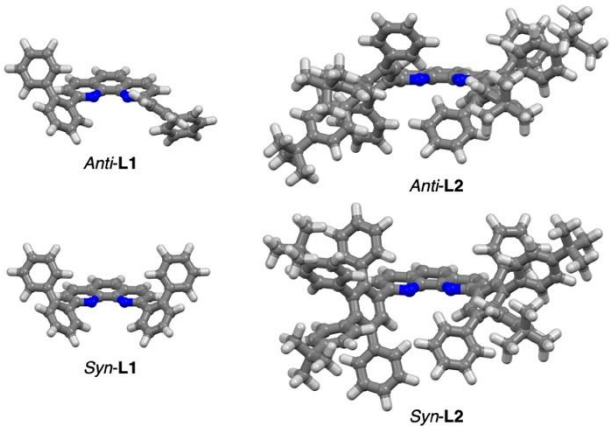

Figure 2. Calculated structures of the C_2-symmetrical *Anti* and C_S-symmetrical *Syn* atropisomers of **L1** and **L2** (conformations minimized at the B3LYP/6-31G* level).

The energy barrier calculated for the rotation about the phenanthroline-phenyl C-C bond in **L1** and **L2** was also evaluated by DFT calculations. In both cases, the rather low calculated energy barriers were fully consistent with the observation of an average NMR spectra even at 203 K (see the Supplementary Information). In the particular case of **L1**, the ^{1}H NMR spectrum recorded at low temperature revealed however the coalescence of the signals corresponding to the biphenyl units (see the Supplementary Information). The energy barrier for the rotation about the C-C bond of the biphenyl moieties of **L1** was effectively estimated significantly higher by DFT calculations (39.5 kJ/mol, see the Supplementary Information). This value is in perfect agreement with the experimental and theoretical data reported by Schlosser and co-workers for the rotational barriers of *ortho*-substituted biphenyl derivatives.[13] At room temperature, the dynamic exchange of the diastereotopic pairs of H-atoms of the biphenyl unit is faster than the NMR timescale and they appear as enantiotopic under these conditions. At 203 K, this exchange is significantly slower explaining the observation of a coalescence. Under our experimental conditions, it was however not possible to record NMR spectra at temperature lower than 203K in order to

observe a fully resolved spectrum showing sharp signals for all the biphenyl signals. A similar behavior was also observed for ligand **L2** due to the restricted rotation about the phenyl-phenyl C-C bonds of the tetraaryl-substituted phenyl subunits (see the Supplementary Information). The calculated energy barriers were fully consistent with the experimental values reported by Gust for hexaarylbenzene derivatives.[14]

Homoleptic copper(I) complexes. Steric constraints are sufficiently important to totally prevent the formation of homoleptic complex $[Cu(\mathbf{L2})_2]^+$ by treatment of **L2** with $[Cu(CH_3CN)_4](BF_4)$. In contrast, a stable homoleptic copper(I) complex was obtained by reaction of **L1** with $[Cu(CH_3CN)_4](BF_4)$ (Scheme 2).

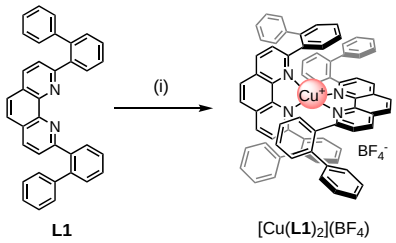

Scheme 2. Preparation of $[Cu(\mathbf{L1})_2](BF_4)$. *Reagents and conditions*: (i) $[Cu(CH_3CN)_4](BF_4)$, CH_3CN/CH_2Cl_2, rt (42%).

Pure $[Cu(\mathbf{L1})_2](BF_4)$ was isolated in 42% yield by column chromatography followed by crystallization in Et_2O/CH_2Cl_2. The MALDI-TOF mass spectrum of $[Cu(\mathbf{L1})_2](BF_4)$ was in full agreement with the proposed structure. Effectively, the expected pseudo-molecular ion peak is observed as the base peak at *m/z* = 1031.3 ($[M\text{-}BF_4^-]^+$, calcd for $C_{72}H_{48}CuN_2$: 1031.32). The absorption spectrum of $[Cu(\mathbf{L1})_2](BF_4)$ also shows the characteristic features of bis-phenanthroline copper(I) complexes[15] with a strong ligand-centered absorption in the UV region and a much weaker band in the visible region (λ_{Max} = 442 nm, ε = 5400 M^{-1} cm^{-1}). The latest is attributed to the metal-to-ligand charge transfer band characteristic of bis-phenanthroline copper(I) complexes and at the origin of their orange-red color.[15] As shown in Figure 3, the ^1H NMR spectrum recorded for $[Cu(\mathbf{L1})_2](BF_4)$ at room temperature exhibits the expected features with the characteristic signals arising from the biphenyl groups as well as two doublets and a singlet for the two equivalent coordinating phenanthroline moieties. However, some signals are broad at room temperature suggesting a dynamic effect. This was confirmed by a variable-temperature NMR study. By increasing the temperature, a perfectly reversible narrowing was observed. At high temperatures, the dynamic exchange between the possible conformers of $[Cu(\mathbf{L1})_2]^+$ is faster than the NMR timescale and the average ^1H NMR spectrum recorded under these conditions is consistent with an apparent D_{2d} symmetry. In contrast, by decreasing the temperature, the dynamic exchange resulting from the rotation around the phenyl-phenanthroline bonds becomes slower as attested by the dramatic broadening of all the signals. At 203 K, the ^1H NMR spectrum is consistent with a mixture of two major atropisomers in a 2:1 ratio but it was difficult to properly assign all the signals. Under these conditions, the major isomer is C_1-symmetrical while the minor has a two-fold symmetry. In order to fully understand the dynamic exchange evidenced by the variable-temperature NMR investigations, a conformational analysis of $[Cu(\mathbf{L1})_2]^+$ was carried out by DFT calculations. As already discussed in the previous section, ligand **L1** may adopt either a C_2-symmetrical *Anti* or a C_s-symmetrical *Syn* conformation. Consequently, the combination of two **L1** moiety around a copper(I) cation can give rise to seven atropisomers (3 pairs of enantiomers and an achiral one, see Figure 4). Conformer **A** combines two *Anti*-**L1** ligands of opposite chirality ([Cu(*S-Anti*-**L1**)(*R-Anti*-**L1**)]$^+$; S_4-symmetrical; achiral). Conformer **B** and its enantiomer ***en*-B** combine one *Syn*-**L1** ligand with an *Anti*-**L1** ligand ([Cu(Syn)(*R*-Anti)]$^+$ and [Cu(*Syn*-**L1**)(*S*-Anti-**L1**)]$^+$; C_1-symmetrical). Conformer **C** and its enantiomer ***en*-C** combine two *Anti*-**L1** ligands of similar chirality ($[Cu(R\text{-}Anti\text{-}\mathbf{L1})_2]^+$ and $[Cu(S\text{-}Anti\text{-}\mathbf{L1})_2]^+$); D_2-symmetrical). Conformer **D** and its enantiomer ***en*-D** combine two *Syn*-**L1** ligands ($[Cu(Syn\text{-}\mathbf{L1})_2]^+$; two possible relative orientations leading to a pair of enantiomers, C_2-symmetrical). DFT calculations revealed that achiral conformer **A** is substantially destabilized by negative steric effects. This is also the case for the D_2-symmetrical conformer (**D**) but to a lesser degree. Finally, the most stable conformers, **B** and **C**, are almost isoenergetic and are expected to be the major species in solution. The Boltzmann distribution calculated from the free energy values of the different isomers shows that the dynamic equilibrium is largely displaced in favor of **B/*en*-B** (63.6%) and **C/*en*-C** (36.2%). This is fully consistent with the NMR data recorded at 203 K. Interconversion between the different isomers occurs by rotation around the phenanthroline-phenyl C-C bonds. The calculated rotational energy barriers are in good agreement with a fast-dynamic exchange between the different conformers at room temperature (Figure 4). These values are also consistent with the observation of isomers in slow exchange on the NMR timescale at 203 K.

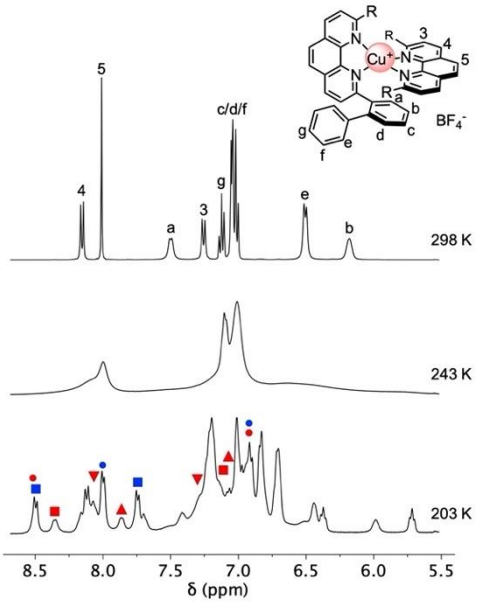

Figure 3. ^1H NMR of $[Cu(\mathbf{L1})_2](BF_4)$ recorded at different temperatures (400 MHz, CD_2Cl_2). At 203 K, four pairs of non-equivalent H(3-4) could be identified for the major C_1-symmetrical atropisomer (indicated in red) and two for the minor D_2-symmetrical one (indicated in blue) with the help of a 2D COSY NMR spectrum.

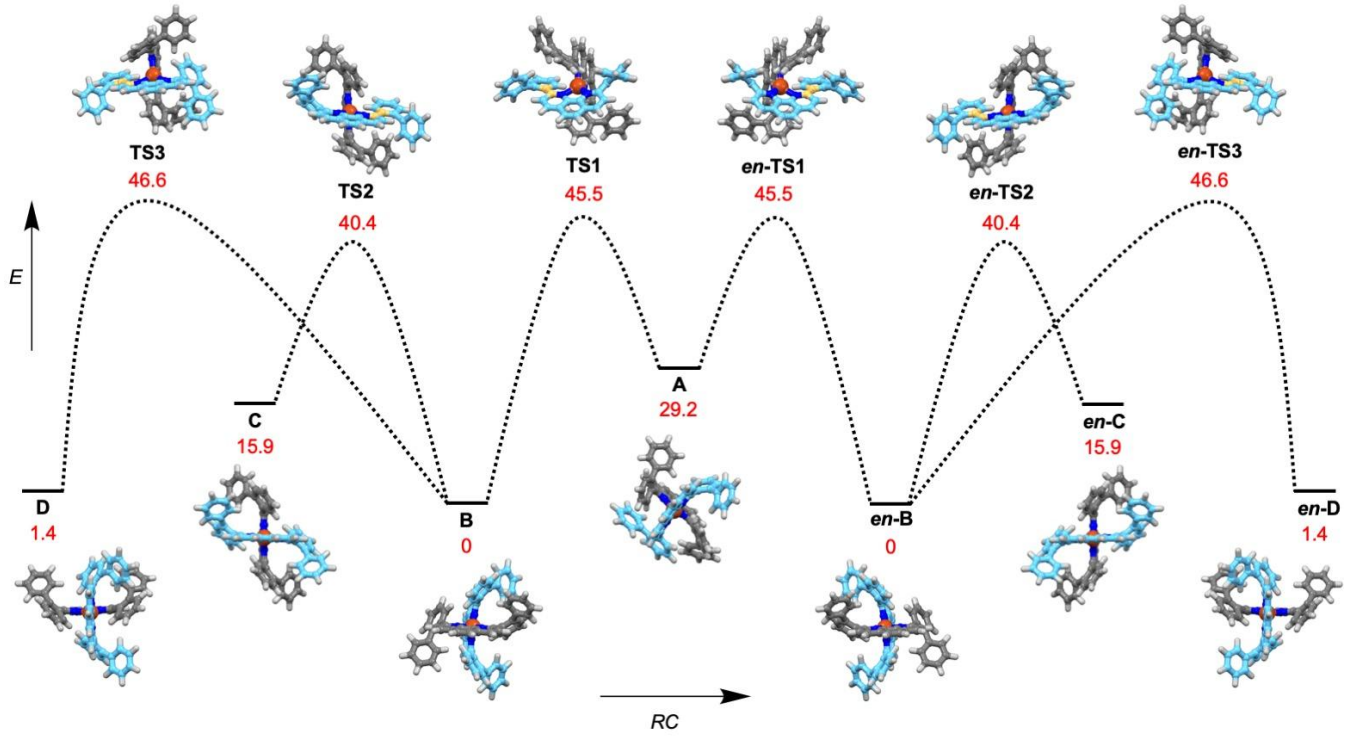

Figure 4. Free energy profile calculated for **[Cu(L1)$_2$]$^+$** at the B3LYP/6-31G* level (relative energies in kJ/mol; for clarity, the C atoms are represented in pale blue for one **L1** ligand and in gray for the second one; the phenyl-phenanthroline C-C bond involved in the isomerization is highlighted in yellow in the transition states). Boltzmann distribution calculated from the computed G^0 values at 298.15 K: **A**: 0.0005%; **B**: 31.8%; ***en*-B**: 31.8%; **C**: 0.05%; ***en*-C**: 0.05%; **D**: 18.1%; ***en*-D**: 18.1%.

Heteroleptic copper(I) complexes. The preparation of heteroleptic copper(I) complexes from **L1** and **L2** is shown in Scheme 3.

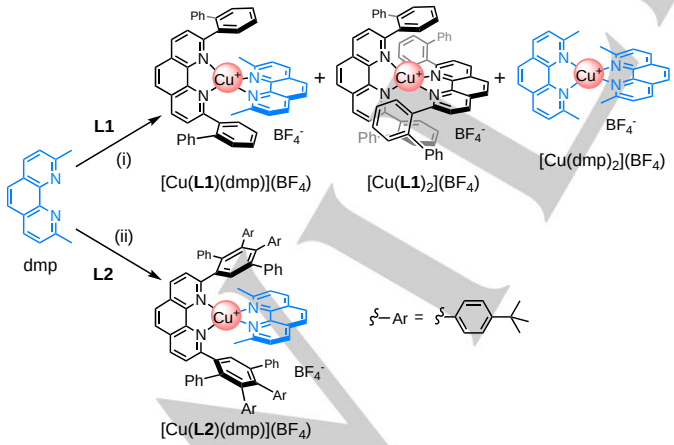

Scheme 3. Preparation of heteroleptic complexes from **L1** and **L2**. *Reagents and conditions*: (i) $[Cu(CH_3CN)_4](BF_4)$, CH_2Cl_2/CH_3CN (the ^{1}H NMR spectrum of the crude mixture revealed the presence of [Cu(**L1**)(dmp)](BF_4), $[Cu(\mathbf{L1})_2](BF_4)$, $[Cu(dmp)_2](BF_4)$ in a 9:1:1 ratio; [Cu(**L1**)(dmp)](BF_4) was isolated pure by crystallization in 62% yield); (ii) $[Cu(CH_3CN)_4](BF_4)$, CH_2Cl_2/CH_3CN (the ^{1}H NMR spectrum of the crude mixture revealed only the presence of [Cu(**L2**)(dmp)](BF_4); [Cu(**L2**)(dmp)](BF_4) was isolated pure by crystallization in 66% yield)

Treatment of **L1** with dmp (1 equiv.) and $[Cu(CH_3CN)_4](BF_4)$ in CH_2Cl_2/CH_3CN gave a mixture of complexes. Analysis of the ^{1}H NMR spectrum recorded in CD_2Cl_2 at rt for the crude mixture revealed the presence of [Cu(**L1**)(dmp)](BF_4), $[Cu(\mathbf{L1})_2](BF_4)$, $[Cu(dmp)_2](BF_4)$ in a 9:1:1 *ratio*. The heteroleptic complex [Cu(**L1**)(dmp)](BF_4) was however isolated pure by slow diffusion of Et_2O into a CH_2Cl_2 solution of the crude mixture. In contrast, the successive addition of **L2** (1 equiv.) and dmp (1 equiv.) to a solution of $[Cu(CH_3CN)_4](BF_4)$ (1 equiv.) in CH_2Cl_2/CH_3CN afforded exclusively the heteroleptic complex [Cu(**L2**)(dmp)](BF_4). In this case, the steric constraints are sufficiently important to totally prevent the formation of $[Cu(\mathbf{L2})_2]^+$ and the coordination scenario is totally driven towards the heteroleptic complex. Recrystallization in Et_2O/CH_2Cl_2 provided pure [Cu(**L2**)(dmp)](BF_4) in 66% yield.

For both [Cu(**L1**)(dmp)](BF_4) and [Cu(**L2**)(dmp)](BF_4), crystals obtained by slow diffusion of Et_2O into a CH_2Cl_2 solution of the complex were suitable for X-ray crystal structure analysis. The structures are shown in Figures 5 and 6. Selected bond lengths and angles are given in Table 1. Two pseudo-C_2 symmetrical $[Cu(\mathbf{L1})(dmp)]^+$ cations are present in the crystal lattice. In both of them, **L1** adopts an *Anti*-conformation (Figure 1A). As a result, the cations are chiral in the solid state and compound [Cu(**L1**)(dmp)](BF_4) crystalized as a racemate. For both cations, the two enantiomers are present in the crystal lattice. They are related by the crystallographic inversion centers (*P*-1 triclinic space group). The coordination about the copper(I) center in

[Cu(**L1**)(dmp)]$^+$ is flattened tetrahedral with angles of 100.6 and 103.7° between the mean planes of the two phenanthroline ligands around Cu(1) and Cu(2), respectively. (Figure 5C). In this way, inter-ligand π-π interactions between dmp and the two biphenyl moieties of **L1** are maximized. A very small rocking of the dmp ligand is also observed, thus explaining the slightly longer C(1)-N(2) and Cu(2)-N(6) bond lengths (Table 1). Detailed inspection of the crystal lattice of [Cu(**L1**)(dmp)](BF$_4$) reveals linear chains alternating cations of opposite chirality in which intermolecular π-stacking interactions between the biphenyl subunits of neighboring cations take place (Figure 5E).

Table 1. Bond length (Å) and bond angles (°) within the coordination spheres for [Cu(**L1**)(dmp)]$^+$ and [Cu(**L2**)(dmp)]$^+$.[a]

	[Cu(**L1**)(dmp)]$^+$	[Cu(**L2**)(dmp)]$^+$
Cu(1)-N(1)	2.031(2)	2.051(4)
Cu(1)-N(2)	2.050(2)	2.027(3)
Cu(1)-N(3)	2.028(3)	2.051(3)
Cu(1)-N(4)	2.025(3)	2.056(3)
N(1)-Cu(1)-N(2)	82.66(8)	83.0(1)
N(1)-Cu(1)-N(3)	120.31(8)	116.2(1)
N(1)-Cu(1)-N(4)	131.82(8)	114.8(1)
N(2)-Cu(1)-N(3)	128.41(8)	137.1(1)
N(2)-Cu(1)-N(4)	116.85(8)	127.4(1)
N(3)-Cu(1)-N(4)	83.14(8)	81.2(1)
Cu(2)-N(5)	2.033(2)	2.057(4)
Cu(2)-N(6)	2.043(2)	2.040(3)
Cu(2)-N(7)	2.025(2)	2.073(3)
Cu(2)-N(8)	2.024(2)	2.056(3)
N(5)-Cu(2)-N(6)	82.67(8)	82.3(1)
N(5)-Cu(2)-N(7)	135.24(8)	112.5(1)
N(5)-Cu(2)-N(8)	116.57(9)	125.2(1)
N(6)-Cu(2)-N(7)	117.44(8)	135.7(1)
N(6)-Cu(1)-N(8)	128.30(9)	124.7(1)
N(7)-Cu(1)-N(8)	83.31(9)	81.9(1)

[a] See Figures 5 and 6 for the numbering.

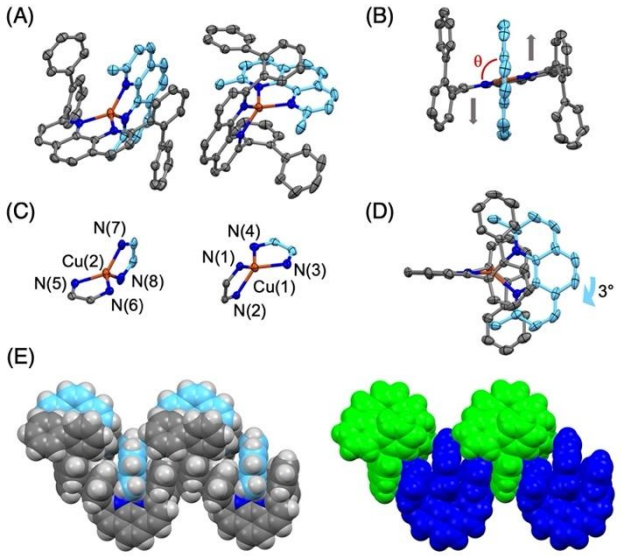

Figure 5. (A) View of the two [Cu(**L1**)(dmp)]$^+$ cations present in the crystal lattice of [Cu(**L1**)(dmp)](BF$_4$).(Et$_2$O); (C) detailed view of the coordination sphere around the Cu(I) centers. Back (B) and side (D) views of [Cu(**L1**)(dmp)]$^+$ highlighting the flattening distortion (angle between the mean planes of **L1** and dmp: θ = 100.6°) of the coordination sphere around Cu(1) and the very limited rocking distortion (ORTEP plots; C: gray for **L1** and pale blue for dmp, N: blue, Cu: orange; the H atoms, the counteranions and the co-crystallized solvent molecules are omitted for clarity; the thermal ellipsoids are shown at the 50% probability level). (E) Stacking within the [Cu(**L1**)(dmp)](BF$_4$).(Et$_2$O) lattice highlighting the intra- and inter-molecular π-π interactions between neighbouring phenanthroline and biphenyl subunit (space filling representations; left: C: gray for **L1** and pale blue for dmp, N: blue, Cu: orange; H: white; right: same view with the cations incorporating Cu(1) in green and Cu(2) in blue).

As shown in Figure 6A, two distinct cations are present in the crystal lattice of [Cu(**L2**)(dmp)](BF$_4$). As observed for the corresponding copper(I) complex obtained from **L1**, ligand **L2** adopts a pseudo-C_2 symmetrical *Anti*-conformation in the [Cu(**L2**)(dmp)]$^+$ cations and compound [Cu(**L2**)(dmp)](BF$_4$) crystallizes as a racemate. The coordination geometry of the copper(I) centers is distorted from a D_{2d} pseudotetrahedral geometry expected for a d^{10} ion.[16] Indeed, a significant rocking distortion is observed (Figure 6C). As a result, the close-to-tetrahedral geometry is distorted towards a trigonal pyramidal geometry. Such a distortion is typically associated with an elongation of the Cu-N bond moving to the axial position.[16] This is not really the case for both [Cu(**L2**)(dmp)]$^+$ cations present in the crystal lattice. On one hand, the copper(I) center is out of the plane of the **L2** ligand by ca. 0.225 Å thus limiting the elongation of the axial Cu-N bond. On the other hand, all the Cu-N bonds are slightly longer than those typically observed for phenanthroline copper(I) complexes.[16] This is ascribed to the steric constraints imposed by the large tetraarylbenzene substituents of **L2**. While an important rocking distortion is observed for the [Cu(**L2**)(dmp)]$^+$ cations, their two phenanthroline moieties are almost perpendicular (Figure 6D).

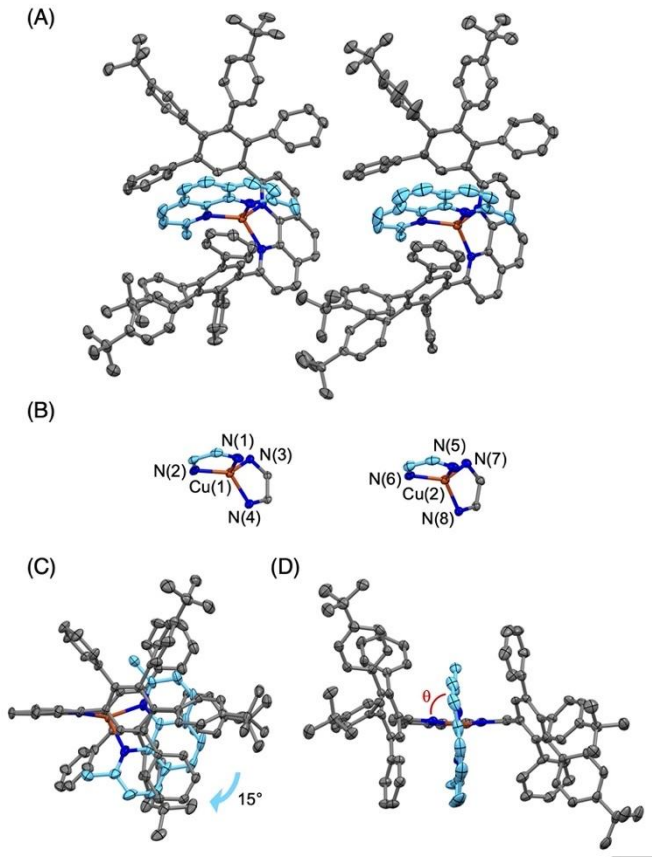

Figure 6. (A) View of the two [Cu(**L2**)(dmp)]$^+$ cations present in the crystal lattice of [Cu(**L1**)(dmp)](BF$_4$).(Et$_2$O) (view along crystallographic *a* axis); (B) detailed view of the coordination sphere around the Cu(I) centers; (C) side and (D) back views of [Cu(**L2**)(dmp)]$^+$ highlighting the rocking distortion of the coordination sphere around Cu(1) and the very limited flattening (angle between the mean planes of **L2** and dmp: θ = 87.1°), (ORTEP plots; C: gray for **L2** and pale blue for dmp, N: blue, Cu: orange; the H atoms and the counteranions are omitted for clarity; the thermal ellipsoids are shown at the 50% probability level).

Both [Cu(**L1**)(dmp)](BF$_4$) and [Cu(**L2**)(dmp)](BF$_4$) are stable in the solid state. Their stability was also evaluated in solution. While CH_2Cl_2 or CH_3CN solutions of [Cu(**L2**)(dmp)](BF$_4$) were stable for days, this was not the case for [Cu(**L1**)(dmp)](BF$_4$). The ^{1}H NMR recorded for a freshly prepared CD_2Cl_2 solution from recrystallized [Cu(**L1**)(dmp)](BF$_4$) revealed the almost exclusive presence of the heteroleptic complex (Figure 7). A very slow evolution was however observed and traces of the homoleptic complexes [Cu(**L1**)$_2$](BF$_4$) and [Cu(dmp)$_2$](BF$_4$) were detected after a few hours. In this solvent, the evolution is extremely slow and the equilibrium is not reached after one week. In contrast, equilibration was found faster in the presence of CH_3CN thus suggesting that this coordinating solvent is catalyzing the ligand exchange reaction.[17] At equilibrium, the ^{1}H NMR spectrum recorded in CD_2Cl_2 revealed the presence of [Cu(**L1**)(dmp)](BF$_4$), [Cu(**L1**)$_2$](BF$_4$) and [Cu(dmp)$_2$](BF$_4$) in a 9:1:1 ratio (Figure 7). The heteroleptic/homoleptic ratio is indeed identical to the one observed in the crude mixture obtained upon mixing **L1**, dmp and [Cu(CH$_3$CN)$_4$](BF$_4$). The proportion of the different species results actually from their relative thermodynamic stability. All these observations revealed that heteroleptic complex [Cu(**L1**)(dmp)](BF$_4$) may be investigated out of equilibrium in CH_2Cl_2 solutions, however one should always consider the slow ligand exchange leading to the formation of the homoleptic complexes.

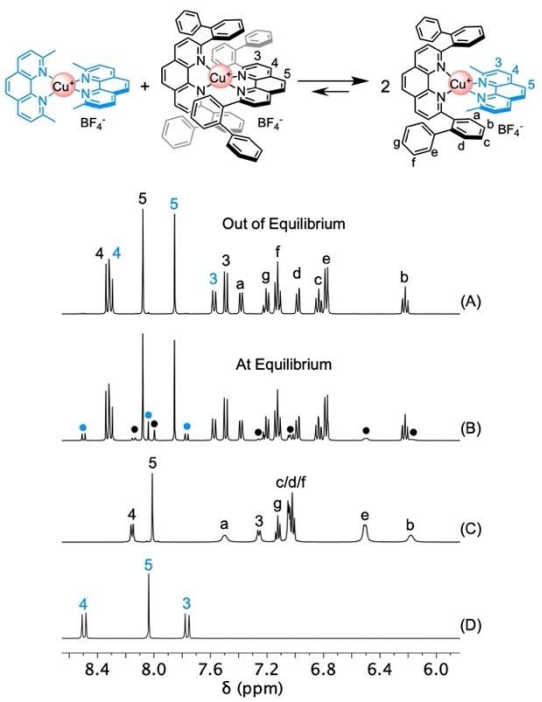

Figure 7. ^{1}H NMR recorded at 298 K for (A) a freshly prepared CD_2Cl_2 solution of [Cu(**L1**)(dmp)](BF$_4$) (out of equilibrium), (B) a CD_2Cl_2 solution of [Cu(**L1**)(dmp)](BF$_4$) in the presence of CH_3CN after the equilibrium was reached (signals corresponding to [Cu(**L1**)$_2$](BF$_4$) are indicated with black marks and those of [Cu(dmp)$_2$](BF$_4$) with blue marks), (C) a CD_2Cl_2 solution of [Cu(**L1**)$_2$](BF$_4$), and (D) a CD_2Cl_2 solution of [Cu(dmp)$_2$](BF$_4$).

In the solid state, only the *Anti* conformers were observed for [Cu(**L1**)(dmp)](BF$_4$) and [Cu(**L2**)(dmp)](BF$_4$). In order to also assess the conformations in solution for these compounds, detailed variable-temperature NMR studies and Density Functional Theory (DFT) calculations were carried out. For both heteroleptic complexes, the *Syn-Anti* isomerization was conveniently monitored by following the evolution of the signals arising from the methyl substituents of the dmp ligand in ^{1}H NMR spectra of [Cu(**L1**)(dmp)](BF$_4$) and [Cu(**L2**)(dmp)](BF$_4$) recorded at different temperatures (Figure 8). At room temperature, the *Syn-Anti* isomerization is faster than the NMR timescale as attested by the observation of a singlet for the methyl groups of dmp in both cases. In contrast at low temperature, the dynamic exchange is slower than the NMR timescale and the two conformers are clearly observed. In both cases, a singlet is observed for the two equivalent methyl groups of the C_2-symmetrical *Anti* conformer, while two singlets are seen for the non-equivalent methyl groups of the C_s-symmetrical *Syn* conformer. The proportion of both conformers is temperature dependent. For [Cu(**L1**)(dmp)](BF$_4$), the *Anti/Syn ratio* estimated from the integration of the CH_3 groups in ^{1}H NMR spectra was *ca*. 6/4 at 243 K and 7/3 at 213 K corresponding to a difference in free energy of *ca*. 1 kJ/mol in favor of the *Anti*-isomer. Similarly, the *Anti/Syn ratio* was *ca*. 94/6 at 243 K and 97/3 at 208 K for [Cu(**L2**)(dmp)](BF$_4$). Based on these values, the

difference in free energy between the *Anti* and the *Syn* conformers was estimated to be *ca*. 6 kJ/mol. By monitoring the coalescence of the H(5) signal from the dmp ligand, the activation free energies for the *Syn-Anti* isomerization through rotation about the phenanthroline-phenyl bond was estimated as $\Delta G^{\ddagger}$ = 48 and 60 kJ/mol for [Cu(**L1**)(dmp)](BF_4) and [Cu(**L2**)(dmp)](BF_4), respectively.

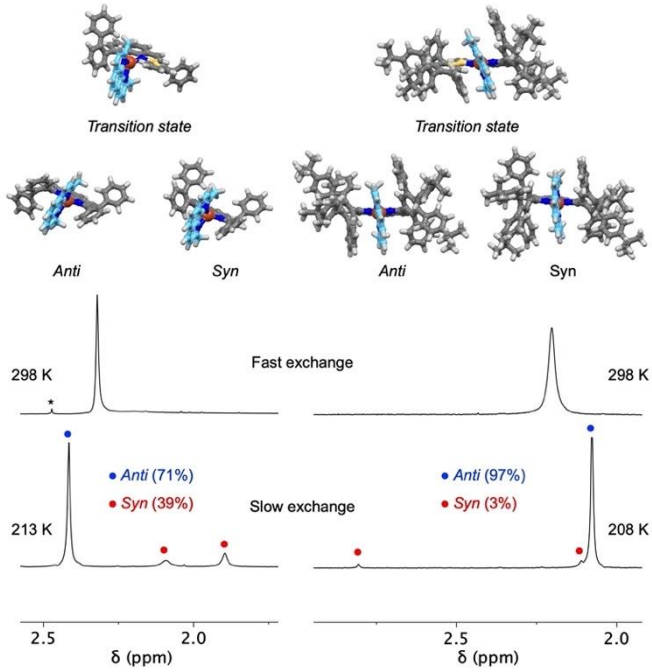

Figure 8. Top: calculated structures of the *Anti* and *Syn* conformers of [Cu(**L1**)(dmp)]$^+$ and [Cu(**L2**)(dmp)]$^+$ as well as the transition states for the *Syn-Anti* isomerizations computed at the B3LYP/6-31G* level in the gas phase (for clarity, the C atoms are represented in pale blue for dmp and in gray for **L1** and **L2**; the phenyl-phenanthroline C-C bond involved in the isomerization is highlighted in yellow in the transition states). Bottom: aliphatic region of the ^{1}H NMR spectra recorded at different temperatures for [Cu(**L1**)(dmp)](BF_4) (left) and [Cu(**L2**)(dmp)](BF_4) (right) showing the resonance of the Me groups of the dmp ligand (* = trace of $[Cu(dmp)_2]^+$).

The *Syn-Anti* isomerization of cations [Cu(**L1**)(dmp)]$^+$ and [Cu(**L2**)(dmp)]$^+$ was also investigated by DFT calculations at the B3LYP/6-31G* level in the gas phase. The calculated *Syn* and *Anti* isomers as well as the transition states for the *Syn-Anti* isomerization through rotation about the phenanthroline-phenyl bond are shown for both heteroleptic copper(I) complexes in Figure 8. The associated total electronic (E) and Gibbs (G^0) energies are given in Table 2. The E values obtained for the *Syn* and *Anti* isomers of [Cu(**L1**)(dmp)]$^+$ are very similar as observed experimentally. There is however a difference of 3.2 kJ/mol between their G^0 values with a preference for the *Syn* isomer. This discrepancy with the experimental data might be ascribed to the idealization of low-frequency vibrators as harmonic oscillators.[13] On the other hand, calculations have been performed in the gas phase. In solution, the relative energy of the two isomers is also influenced by their dipole moments. The significant difference (*ca*. 1.7 D) between the calculated dipole moments of the *Syn* and *Anti* isomers may also influence their behavior in solution. As one may expect, it appears that the most abundant conformer in CD_2Cl_2 is the one having the smallest dipole moment. In the case of [Cu(**L2**)(dmp)]$^+$, the relative E and G^0 values between the two conformers revealed a clear preference for the *Anti*. The *Syn* conformer is clearly destabilized by steric factors and this is in perfect agreement with our experimental observations. Finally, the computed free energy barriers for the *Syn/Anti* isomerizations are in good agreement with experimental values obtained by the variable-temperature NMR data for both [Cu(**L1**)(dmp)]$^+$ and [Cu(**L2**)(dmp)]$^+$.

Table 2. Total electronic energies (E) and Gibbs energies at 298.15 K (G^0) for the *Anti* and *Syn* conformers of [Cu(**L1**)(dmp)]$^+$ and [Cu(**L2**)(dmp)]$^+$ as well as the transition states (*TS*) for the *Syn-Anti* isomerizations computed at the B3LYP/6-31G* level in the gas phase.[a]

	E (Hartree)	Relative E (kJ/mol)	G^0 (Hartree)	ΔG^0 (kJ/mol)
		[Cu(**L1**)(dmp)]$^+$		
Anti	-3786.326910	0.3	-3785.726125	3.2[b]
Syn	-3786.327019	0	-3785.727352	0[b]
TS	-3786.314321	33.3	-3785.709887	45.8
		[Cu(**L2**)(dmp)]$^+$		
Anti	-5801.657948	0	-5800.237871	0[c]
Syn	-5801.652126	15.3	-5800.232074	15.2[c]
TS	-5801.637529	53.6	-5800.216821	55.3

[a] The calculated structures are shown in Figure 8. [b] Boltzmann distribution calculated from the computed G^0 values at 298.15 K: *Anti*: 21.4%; *Syn*: 78.6%. [c] Boltzmann distribution calculated from the computed G^0 values at 298.15 K: *Anti*: 99.8%; *Syn*: 0.2%.

DFT studies of the equilibrium between homo- and heteroleptic copper(I) complexes. In order to evaluate the steric constrains of the different ligands discussed in the present paper, the equilibrium between [Cu(L)(dmp)]$^+$ (L = **L1**, **L2** or dMesp) and the corresponding homoleptic complexes was analyzed by theoretical calculations. The computed free energy values and the corresponding Boltzmann distributions obtained at the B3LYP/6-31G* level in the gas phase are summarized in Table 3. It can be noted that the same calculations were also done at the semi-empirical PM6 level (see the Supplementary Information). The PM6 level is actually sufficient to rapidly evaluate the possibility to prepare stable heteroleptic copper(I) complexes from two ligands, however the calculated ΔG^0 values for the homoleptic/heteroleptic equilibrium are clearly underestimated. In contrast, the ΔG^0 obtained at the B3LYP/6-31G* level are most likely overestimated but the comparison between the values obtained for the different systems provides a good estimation of the relative steric constraints resulting from the nature of the L ligand. In the case of **L1**, the biphenyl group is not sufficiently large to prevent the formation of the homoleptic complex. Accordingly, a relatively modest ΔG^0 value was calculated for the homoleptic/heteroleptic equilibrium (-13.2 kJ/mol). In contrast, the large ΔG^0 values calculated in the case of **L2** and dMesp are in good agreement with the experimental observations. Effectively, the steric constraints are sufficiently important in both cases to prevent the formation of the corresponding homoleptic complexes and their associated high

energy contributes largely to favor the heteroleptic complex. In this case, the steric constraints are minimized as the second ligand, namely dmp, is not substituted with sterically demanding groups. Comparison of **L1** and **L2** shows that the three additional aryl substituents on each phenyl units attached to the phenanthroline core play a key role in the steric destabilization of the homoleptic complex with an energy penalty of 144.7 kJ/mol. In this way, their presence contributes to favor the formation of the heteroleptic complex. However, the unsubstituted *ortho*-position led to a reduced steric constraints of 65.1 kJ/mol when compared to dMesp in which the two *ortho*-positions are substituted. It is also known that replacing the Me groups of dMesp by larger *i*-Pr substituents generates enormous steric constraints that also destabilize the heteroleptic complex.[18] As a result, the latest is not stable and decoordination is observed in solution. The present results show that using mono-substituted ortho-phenyl groups is an appealing strategy to further increase the steric demand without destabilizing the heteroleptic complex. This is extremely important in the perspective of future developments of strongly luminescent copper(I) complexes as increased steric constraint prevents severe distortion of the coordination sphere in the excited state.[15]

Table 3. Relative Gibbs energies at 298.15 K (G^0) for $[Cu(dmp)_2]^+ + [Cu(L)_2]^+ \rightleftarrows 2\ [Cu(dmp)(L)]^+$ computed at the B3LYP/6-31G* level in the gas phase. The Boltzmann distributions have been calculated based on the ΔG^0 values at 298.15 K.

	Relative G^0 (kJ/mol)	Boltzmann distribution
	$[Cu(dmp)_2]^+ + [Cu(\mathbf{L1})_2]^+ \rightleftarrows 2\ [Cu(dmp)(\mathbf{L1})]^+$	
$[Cu(dmp)_2]^+ + [Cu(\mathbf{L1})_2]^+$	0	0.5%
$2\ [Cu(dmp)(\mathbf{L1})]^+$	-13.2	99.5%
	$[Cu(dmp)_2]^+ + [Cu(\mathbf{L2})_2]^+ \rightleftarrows 2\ [Cu(dmp)(\mathbf{L2})]^+$	
$[Cu(dmp)_2]^+ + [Cu(\mathbf{L2})_2]^+$	0	0
$[2\ [Cu(dmp)(\mathbf{L2})]^+$	-157.9	100%
	$[Cu(dmp)_2]^+ + [Cu(dMesp)_2]^+ \rightleftarrows 2\ [Cu(dmp)(dMesp)]^+$	
$[Cu(dMesp)_2]^+ + [Cu(L)_2]^+$	0	0
$2\ [Cu(dmp)(dMesp)]^+$	-223.0	100%

Conclusion

Two phenanthroline ligands substituted in their 2,9-positions with mono- and tetra-arylated phenyl groups have been prepared. In the case of the tetraarylphenyl-substituted ligand (**L2**), steric effects totally prevent the formation of a bis-phenanthroline copper(I) compex. In contrast, the steric constraints resulting from the presence of two biphenyl substituents in **L1** are not sufficient to prevent the formation of a stable homoleptic copper(I) complex. Owing to the possible relative *Syn* and *Anti* orientation of the two biphenyl moieties in **L1**, a complicated conformational equilibrium has been evidenced for the resulting homoleptic copper(I) complex. Detailed dynamic NMR studies combined with DFT calculations have shown that the dynamic conformational equilibrium favors two specific conformers out of the four possible ones. Both **L1** and **L2** have been also combined with dmp to generate the corresponding heteroleptic copper(I) complexes. Owing to limited steric constraints, the homoleptic/heteroleptic equilibrium is not totally displaced in favor of [Cu(**L1**)(dmp)](BF_4). This compound has been however isolated pure in the solid state by crystallization. When dissolved in a non-coordinating solvent, the ligand exchange reaction is very slow and [Cu(**L1**)(dmp)](BF_4) can be investigated out of equilibrium. In contrast, in coordinating solvents, the ligand exchange reaction is fast and a thermodynamic equilibrium is rapidly reached. The proportion of the different species, namely [Cu(**L1**)(dmp)](BF_4), [Cu(**L1**)$_2$](BF_4) and [Cu(dmp)$_2$](BF_4), results from their relative thermodynamic stability. In the case of **L2**, the steric constraints are sufficiently important to completely drive the coordination scenario towards the exclusive formation of [Cu(**L1**)(dmp)](BF_4). Interestingly, only the *Anti* conformers have been observed in the solid state for both [Cu(**L1**)(dmp)](BF_4) and [Cu(**L2**)(dmp)](BF_4). In contrast, detailed NMR studies have shown a dynamic *Syn/Anti* conformational equilibrium in solution. DFT calculations have been useful to fully elucidate the conformational equilibrium observed for the copper(I) complexes reported in this study. They are also helpful to assess the steric constraints in such compounds and are thus essential in the design of stable heteroleptic bis-phenanthroline copper(I) complexes. The principle design reported herein will be further investigated, in particular for the development of new copper(I) photocatalysts. Work in this direction is underway in our laboratory.

Experimental Section

General. Reagents (reagent grade) and solvents (analytical grade) were purchased and used without further purification. Compounds **3**,[11] **4**,[12] and [Cu(dmp)$_2$](BF_4)[19] were prepared according to literature procedures. All reactions were performed in standard glassware under an inert argon atmosphere. Column chromatography: silica gel 60 (70-230 mesh, 0.063-0.200 mm) was purchased from E. Merck. Thin-layer chromatography (TLC) was performed on aluminium sheets coated with silica gel 60 F254 purchased from E. Merck, visualization was done by irradiation with UV light. Melting points (M.p.) were measured on a Gallenkamp melting point apparatus. IR spectra (cm^{-1}) were measured on a Perkin Elmer Spectrum 2 instrument. UV/Vis spectra have been recorded on a Perkin Elmer spectrophotometer Lambda 365 (λ_{max} in nm, ε in $M^{-1}\ cm^{-1}$). NMR spectra were recorded on a Bruker Avance I (300 MHz), Bruker Avance III HD (400 MHz) or a Bruker Avance III HD (500 MHz) with solvent peaks as reference and at 298 K if not indicated otherwise (br: broad signal).). MALDI-TOF-mass spectra (m/z, % relative intensity) were carried out on a Bruker ULTRAFLEX^{TM} matrix-assisted laser desorption ionization time-of-flight mass spectrometer. A saturated solution of 1,8,9-anthracenetriol (dithranol, ALDRICH) in CH_2Cl_2 was used as matrix. Elemental analyses were performed on a Flash 2000 apparatus of ThermoFisher Scientific at the Analytical Service of the University of Strasbourg, France.

Compound 2. *n*-BuLi (1.6M in hexanes, 2.14 mL, 3.43 mmol) was added slowly to a solution of **1** (800 mg, 3.43 mmol) in dry diethyl ether (20 mL) under argon at 0°C. After 10 min, the solution was allowed to warm to rt and stirring was continued at rt for 2h. This solution was then transferred slowly over 15 min to a suspension of 1,10-phenanthroline (309 mg, 1.72 mmol) in dry diethyl ether (15 mL) under argon and at 0°C. The resulting red reaction mixture was allowed to warm to rt and stirring was continued

for 4 h. A saturated aqueous NH_4Cl solution (5 mL) was added, the organic phase separated, and the aqueous phase extracted with CH_2Cl_2 (2x10 mL). The combined organic phases were washed with H_2O (10 mL) and brine (10 mL), dried with Na_2SO_4 and evaporated. The crude was dissolved in CH_2Cl_2 (20 mL), MnO_2 (3.00 g, 3.44 mmol) was added and the mixture stirred at rt for 2 h. The mixture was filtered over celite (CH_2Cl_2) and evaporated. Column chromatography (SiO_2; eluent: CH_2Cl_2 to CH_2Cl_2/MeOH 50:1) gave **2** (410 mg, 72%). Highly viscous pale-yellow oil. IR (neat, cm^{-1}): ν = 3042, 1487, 851, 746, 701; ^{1}H NMR (500 MHz, $CDCl_3$): δ = 9.28 (dd, *J* = 4, 1 Hz, 1H), 8.28 (dd, *J* = 8, 2 Hz, 1H), 8.13-8.06 (m, 1H), 7.86 (d, *J* = 8 Hz, 1H), 7.78 (d, *J* = 9 Hz, 1H), 7.72 (d, *J* = 9 Hz, 1H), 7.65 (dd, *J* = 8, 4 Hz, 1H), 7.13 (d, *J* = 8 Hz, 1H) ppm; ^{13}C NMR (126 MHz, $CDCl_3$): δ = 160.1, 150.4, 146.3, 146.2, 141.4, 140.6, 140.1, 136.3, 134.8, 132.1, 130.3, 130.1, 129.0, 128.9, 128.3, 128.0, 127.0, 126.9, 126.6, 126.3, 125.7, 122.9 ppm; Elemental analysis calcd. for $C_{24}H_{16}N_2$ x 2/3 CH_2Cl_2: C 76.16, H 4.49, N 7.20; found: C 75.99, H 4.46, N 7.21; MALDI-TOF MS (m/z): 333.16 ($[M+H]^+$, calcd for $C_{24}H_{17}N_2$: 333.14).

Ligand L1. *n*-BuLi (1.6M in hexanes, 2.14 mL, 3.43 mmol) was added slowly to a solution of **1** (800 mg, 3.43 mmol) in dry diethyl ether (20 mL) under argon at 0°C. After 10 min, the solution was allowed to warm to rt and stirring was continued at rt for 2h. This solution was then transferred slowly over 20 min to a suspension of **2** (570 mg, 1.72 mmol) in dry diethyl ether (25 mL) under argon and at 0°C. The resulting purple reaction mixture was allowed to warm to rt and stirring was continued for 17 h. A saturated aqueous NH_4Cl solution (15 mL) was added, the organic phase separated, and the aqueous phase extracted with CH_2Cl_2 (10 mL). The combined organic phases were washed with brine (10 mL), dried with Na_2SO_4 and evaporated. The crude was dissolved in CH_2Cl_2 (20 mL), MnO_2 (3.00 g, 3.44 mmol) was added and the mixture stirred at rt for 2 h. The mixture was filtered over celite (CH_2Cl_2) and evaporated. Column chromatography (SiO_2; eluent: cyclohexane / diethylether 4:1 to 3:1) gave **L1** (680 mg, 82%). Colorless solid. M.p.: 109-110°C; IR (neat, cm^{-1}): ν = 3055, 1492, 1476, 855, 745, 701; ^{1}H NMR (500 MHz, CD_2Cl_2): δ = 8.00 (dd, *J* = 4, 1 Hz, 2H), 7.91 (d, *J* = 8 Hz, 2H), 7.70 (s, 2H), 7.58 (m, 4H), 7.54 (m, 2H), 7.30 (m, 4H), 7.23 (m, 6H), 7.20 (d, *J* = 8 Hz, 2H) ppm; ^{13}C NMR (126 MHz, CD_2Cl_2): δ = 159.9, 146.8, 142.0, 141.5, 140.6, 135.4, 132.0, 131.1, 130.6, 129.3, 128.6, 128.3, 127.6, 127.3, 126.7, 125.5 ppm; Elemental analysis calcd. for $C_{36}H_{24}N_2$xC_6H_{14}: C 88.38, H 6.71, N 4.91; found: C 88.33, H 5.81, N 5.30; MALDI-TOF MS (m/z): 485.13 ($[M+H]^+$, calcd for $C_{36}H_{25}N_2$: 485.20).

Ligand L2. A mixture of **3** (159.2 mg, 0.70 mmol) and **4** (762.2 mg, 1.54 mmol) in *o*-xylene (10 ml) was heated at 80°C under argon for 30 min. The temperature was slowly raised to reflux within 1h and the mixture kept at reflux overnight. The solvent was removed by using a gentle stream of air while heating at 100°C and the resulting solid was further dried under high vacuum. Column chromatography (SiO_2; eluent: CH_2Cl_2/MeOH 100:1 to 20:1) gave **L2** (582 mg, 71%). Beige solid. M.p.: 207-208°C; IR (neat, cm^{-1}): ν = 2960, 1495, 838, 699; UV/Vis (CH_2Cl_2): λ_{max} (ε, M^{-1} cm^{-1}) = 246 (121300), 285 (sh, 58600), 310 (sh, 43300), 355 (sh, 5100); ^{1}H NMR (300 MHz, CD_2Cl_2): δ = 7.89 (d, *J* = 8 Hz, 2H), 7.84 (s, 2H), 7.65 (s, 2H), 7.27 (d, *J* = 8 Hz, 2H), 7.24 (m, 4H), 7.13 (m, 6H), 7.01 (m, 4H), 6.96 (AB system, 4H), 6.90 (AB system, 4H), 6.84-6.88 (m, 2H), 6.78-6.83 (m, 8H), 6.74 (AB system, 4H), 1.17 (s, 18H, *t*Bu), 1.15 (s, 18H, *t*Bu) ppm; ^{13}C NMR (126 MHz, CD_2Cl_2): δ = 160.4, 149.0, 148.7, 146.4, 142.7, 142.6, 141.5, 141.4, 141.0, 140.7, 139.9, 137.9, 137.8, 135.2, 132.3, 131.7, 131.7, 131.6, 130.6, 128.0, 127.4, 127.3, 126.7, 126.5, 126.1, 125.1, 124.1, 123.8, 34.6, 34.6, 31.5, 31.5 ppm; Elemental analysis calcd. for $C_{88}H_{80}N_2$•1/3CH_2Cl_2: C 88.86, H 6.81, N 2.35; found: C 88.56, H 6.75, N 2.35; MALDI-TOF MS (m/z): 1165.46 ($[M+H]^+$, calcd for $C_{88}H_{81}N_2$: 1165.64).

[Cu(L1)$_2$](BF$_4$). A solution of **L1** (150 mg, 0.309 mmol) in CH_2Cl_2 (15 mL) was added to a solution of $[Cu(CH_3CN)_4](BF_4)$ (48.6 mg, 0.155 mmol) in MeCN (15 mL) under argon. The resulting orange solution was stirred for 1 h at rt and evaporated. Column chromatography (SiO_2; eluent: CH_2Cl_2 to CH_2Cl_2/MeOH 80:1 to 50:1) followed by crystallization from CH_2Cl_2/diethyl ether gave [Cu(**L1**)$_2$](BF$_4$) (72.8 mg, 42%). Dark orange-red solid. M.p.: 184-186°C; IR (neat, cm^{-1}): ν = 3058, 1494, 1477, 1054, 861, 743, 701; UV/Vis (CH_2Cl_2): λ_{max} (ε, M^{-1} cm^{-1}) = 319 (59200), 442 (5400); ^{1}H NMR (500 MHz, CD_2Cl_2): δ = 8.15 (d, *J* = 8 Hz, 4H), 8.01 (s, 4H), 7.50 (br s, 4H), 7.26 (d, *J* = 8 Hz, 4H), 7.12 (m, 4H), 7.07-6.97 (m, 16H), 6.51 (d, *J* = 8 Hz, 8H), 6.18 (br s, 4H) ppm; ^{13}C NMR (126 MHz, CD_2Cl_2): δ = 158.5, 144.4, 141.6, 140.1, 138.1, 136.5, 130.9, 130.1, 129.8, 129.2, 128.9, 128.7, 127.8, 127.6, 126.2 ppm; Elemental analysis calcd. for $C_{72}H_{48}BCuF_4N_4$ x 1/3 CH_2Cl_2: C 75.69, H 4.28, N 4.88; found: C 75.44, H 4.41, N 4.80; MALDI-TOF MS (m/z): 1031.31 ($[M\text{-}BF_4^-]^+$, calcd for $C_{72}H_{48}CuN_2$: 1031.32).

[Cu(L1)(dmp)](BF$_4$). A solution of **L1** (100 mg, 0.206 mmol) in CH_2Cl_2 (5 mL) was added to a solution of $[Cu(CH_3CN)_4]BF_4$ (64.9 mg, 0.206 mmol) in MeCN (5 mL) under argon. The solution turned yellow. After 10 min, a solution of dmp (43.0 mg, 0.206 mmol) in CH_2Cl_2 (5 mL) was added. The resulting red solution was stirred for 1 h at rt and evaporated. Crystallization from CH_2Cl_2/diethyl ether gave [Cu(**L1**)(dmp)](BF$_4$) (107.9 mg, 62%). M.p.: 148-149°C; Dark red solid. IR (neat, cm^{-1}): ν = 3059, 1494, 1477, 1051, 1035, 859, 743, 729, 701; UV/Vis (CH_2Cl_2): λ_{max} (ε, M^{-1} cm^{-1}) = 275 (39900), 295 (sh, 35000), 310 (sh, 28000), 461 (5200);; ^{1}H NMR (400 MHz, CD_2Cl_2): δ = 8.33 (d, *J* = 8 Hz, 4H), 8.30 (d, *J* = 8 Hz, 4H), 8.08 (s, 2H), 7.85 (s, 2H), 7.57 (d, *J* = 8 Hz, 2H), 7.49 (d, *J* = 8 Hz, 2H), 7.38 (dd, *J* = 8, 1 Hz, 2H), 7.20 (m, 2H), 7.12 (m, 4H), 6.98 (dd, *J* = 8, 1 Hz, 2H), 6.84 (td, *J* = 8, 1 Hz, 2H), 6.78 (m, 4H), 6.22 (td, *J* = 8, 1 Hz, 2H), 2.28 (s, 6H) ppm; MALDI-TOF MS (m/z): 755.22 ($[M\text{-}BF_4]^+$, calcd for $C_{50}H_{36}CuN_4$: 755.22).

[Cu(L2)(dmp)](BF$_4$). A solution of **L2** (100 mg, 0.086 mmol) in CH_2Cl_2 (5 mL) was added to a solution of $[Cu(CH_3CN)_4]BF_4$ (27.0 mg, 0.086 mmol) in MeCN (5 mL) under argon. The solution turned yellow. After 10 min, a solution of dmp (17.9 mg, 0.086 mmol) in CH_2Cl_2 (5 mL) was added. The resulting red solution was stirred for 1 h at rt. The resulting red solution was stirred for 1 h at rt and evaporated. Crystallization from CH_2Cl_2/diethyl ether gave [Cu(**L2**)(dmp)](BF$_4$) (86 mg, 66%). Red crystalline solid. M.p.: >300°C; IR (neat, cm^{-1}): ν = 2960, 1500, 1056, 857, 839, 701; UV/Vis (CH_2Cl_2): λ_{max} (ε, M^{-1} cm^{-1}) = 253 (100500), 320 (sh, 35000), 453 (4800); ^{1}H NMR (500 MHz, CD_2Cl_2): δ = 8.17 (d, *J* = 8 Hz, 2H), 8.07 (br s, 2H), 8.01 (s, 2H), 7.75 (br s, 2H), 7.69 (br s, 2H), 7.30 (br s, 2H), 7.25 (br m, 2H), 6.97 (m, 4H), 6.72-88 (br m, 14H), 6.70 (m, 4H), 6.40 (br s, 4H), 6.17 (br d, *J* = 8 Hz, 4H), 6.02 (br s, 2H), 5.96 (br s, 2H), 5.90 (br s, 2H), 2.20 (s, 6H), 1.11 (s, 18H), 1.08 (s, 18H) ppm; ^{1}H NMR (400 MHz, CD_2Cl_2, -40°C): δ = 8.15 (d, *J* = 8 Hz, 2H), 8.06 (d, *J* = 8 Hz, 2H), 7.99 (s, 2H), 7.73 (s, 2H), 7.67 (s, 2H), 7.27 (d, *J* = 8 Hz, 2H), 7.15 (d, *J* = 8 Hz, 2H), 6.95 (m, 4H), 6.72-6.85 (m, 12H), 6.67 (m, 6H), 6.37 (dd, *J* = 8, 2 Hz, 2H), 6.34 (dd, *J* = 8, 2 Hz, 2H), 6.13 (d, *J* = 8 Hz, 4H), 5.92 (d, *J* = 8 Hz, 4H), 5.89 (dd, *J* = 8, 2 Hz, 2H), 5.84 (dd, *J* = 8, 2 Hz, 2H), 2.11 (s, 6H), 1.06 (s, 18H), 1.03 (s, 18H) ppm; ^{13}C NMR (126 MHz, CD_2Cl_2): δ = 159.4, 157.1, 149.4, 149.0, 144.4, 143.1, 142.4, 141.7, 139.8, 139.4, 139.3, 139.2, 138.8, 137.2, 136.8, 136.7, 136.2, 132.3, 131.6, 131.1, 130.8, 130.4, 129.5, 128.2, 128.1, 127.5, 127.5, 127.3, 127.0, 126.6, 126.2, 125.7, 124.2, 124.1, 123.6, 34.6, 34.5, 31.5, 31.4, 25.9 ppm; Elemental analysis calcd. for $C_{102}H_{92}BCuF_4N_4$ x 1/5 CH_2Cl_2: C 79.65, H 6.04, N 3.64; found: C 79.74, H 6.13, N 3.71; MALDI-TOF MS (m/z): 1435.62 ($[M\text{-}BF_4]^+$, calcd for $C_{102}H_{92}CuN_4$: 1435.66).

X-ray crystal structures. The crystallographic data and the refinement parameters are reported in the Supporting Information for all the compounds. The X-ray crystal structures have been deposited at the Cambridge Structural Database (CCDC deposition numbers: 2079617 for [Cu(**L1**)(dmp)](BF$_4$) and 2079620 for [Cu(**L2**)(dmp)](BF$_4$)). These data are provided free of charge by the joint Cambridge Crystallographic Data Centre and Fachinformationszentrum Karlsruhe Access Structures service (https://www.ccdc.cam.ac.uk/structures).

Acknowledgements

Financial support by the International Center for Frontier Research in Chemistry and the LabEx “Chimie des Systèmes Complexes” is gratefully acknowledged. We thank L. Karmazin and C. Bailly for the X-ray crystal structure resolutions and J.-M. Strub for the mass spectra.

Keywords: Conformation • Copper • Dynamic NMR studies • Heteroleptic complexes • Phenanthroline

[1] a) A. J. McConnel, C. S. Wood, P. P. Neelakanda, J. R. Nitschke, *Chem. Rev*. **2015**, *115*, 7729-7793. b) S. E. Howson, P. Scvott, *Dalton Trans*. **2011**, *40*, 10268-10277. c) J.-M. Lehn, *Supramolecular Chemistry, Concepts and Perspectives*, VCH, Weinheim, 1995. d) V. G. Machado, P. N. W. Baxter, J.-M. Lehn, *J. Braz. Chem. Soc*. **2001**, *12*, 431-462.

[2] a) J.-M. Lehn, A. Rigault, J. Siegel, J. Harrowfield, B. Chevrier, D. Moras, *Proc. Natl. Acad. Sci. USA* **1987**, *84*, 2565-2569. b) J.-M. Lehn, A. Rigault, *Angew. Chem. Int. Ed*. **1988**, *27*, 1095-1097. c) E. C. Constable, M. J. Hannon, A. J. Edwards, P. R. Raithby, *J. Chem. Soc., Dalton Trans*. **1994**, 2669-2677. d) E. C. Constable, S. M. Elder, M. J. Hannon, A. Martin, P. R. Raithby, D. A. Tocher, *J. Chem. Soc., Dalton Trans*. **1996**, 2423-2433. e) E. C. Constable, F. Heirtzler, M. Neuburger, M. Zehnder, *J. Am. Chem. Soc*. **1997**, *119*, 5606-5617.

[3] A. Marquis-Rigault, A. Dupont-Gervais, P. N. W. Baxter, A. Van Dorsselaer, J.-M. Lehn, *Inorg. Chem*. **1996**, *35*, 2307-2310.

[4] a) L. N. Dawe, T. S. M. Abedin, L. K. Thompson, *Dalton Trans*. **2008**, 1661-1675 and references therein. b) S. Toyota, C. R. Woods, M. Benaglia, R. Haldimann, K. Wärnmark, K. Hardcastle, J. S. Siegel, *Angew. Chem. Int. Ed*. **2001**, *40*, 751-754.

[5] a) S. De, K. Mahata, M. Schmittel, *Chem. Soc. Rev*. **2010**, *39*, 1555-1575. b) M. Holler, B. Delavaux-Nicot, J.-F. Nierengarten, *Chem. Eur. J.* **2019**, *25*, 4543-4550.

[6] a) C. O. Dietrich-Buchecker, J.-P. Sauvage, J.-P. Kintzinger, *Tetrahedron Lett.* **1983**, *24*, 5095-5098. b) C. O. Dietrich-Buchecker, J.-P. Sauvage, *Tetrahedron* **1990**, *46*, 503-512.

[7] a) M. Schmittel, A. Ganz, *Chem. Commun*. **1997**, 999-1000. b) M. T. Miller, P. K. Gantzel, T. B. Karpishin, *J. Am. Chem. Soc*. **1999**, *121*, 4292-4293. c) M. Schmittel, A. Ganz, D. Fenske, *Org. Lett*. **2002**, *4*, 2289-2292. d) M. Schmittel, H. Ammon, V. Kalsani, A. Wiegrefe, C. Michel, *Chem. Commun*. **2002**, 2566-2567. e) V. Kalsani, H. Amon, F. Jäckel, J. P. Rabe, M. Schmittel, *Chem. Eur. J*. **2004**, *10*, 5481-5492.

[8] a) R. Krämer, J.-M. Lehn, A.-M. Marquis-Rigault, *Proc. Natl. Acad. Sci. USA* **1993**, *90*, 5394-5398. b) M. Albrecht, *Chem. Rev*. **2001**, *101*, 3457-3498. c) R. Chakrabarty, P. S. Mukherjee, P. J. Stang, *Chem. Rev.* **2011**, *111*, 6810-6918. (d) M. Fujita, *Chem. Soc. Rev*. **1998**, *27*, 417-425.

[9] P. A. Marnot,, C. O. Dietrich-Buchecker, J.-P. Sauvage, *Tetrahedron Lett.* **1982**, *23*, 5291-5294.

[10] J. Wu, W. Pisula, K. Müllen, *Chem. Rev*. **2007**, *107*, 718-747.

[11] R. Ziessel, J. Suffert, M.-T. Youninou, *J. Org. Chem.* **1996**, *61*, 6535-6546.

[12] K. R. J. Thomas, M. Velusamy, J. T. Lin, C. H. Chuen, Y.-T. Tao, *J. Mater. Chem.* **2005**, *15*, 4453-4459.

[13] a) R. Ruzziconi, S. Spizzichino, L. Lunazzi, A. Mazzanti, M. Schlosser, *Chem. Eur. J*. **2009**, *15*, 2645-2652. b) R. Ruzziconi, S. Spizzichino, A. Mazzanti, L. Lunazzi, M. Schlosser, *Org. Biomol. Chem*. **2010**, *8*, 4463-4471. c) A. Mazzanti, L. Lunazzi, R. Ruzziconi, S. Spizzichino, M. Schlosser, *Chem. Eur. J*. **2010**, *16*, 9186-9192. d) L. Lunazzi, M. Mancinelli, A. Mazzanti, S. Lepri, R. Ruzziconi, M. Schlosser, *Org. Biomol. Chem*. **2012**, *10*, 1847-1855.

[14] D. Gust, *J. Am. Chem. Soc*. **1977**, *99*, 6980-6982.

[15] M. Ruthkosky, C. A. Kelly, F. N. Castellano, G. J. Meyer, *Coord. Chem. Rev.* **1998**, *171*, 309-322.

[16] a) D. A. Bardwell, A. M. W. Cargill Thompson, J. C. Jeffery, E. E. M. Tilley, M. D. Ward, *J. Chem. Soc., Dalton Trans.* **1995**, 835-841. b) M. T. Miller, P. K. Gantzel, T. B. Karpishin, *Inorg. Chem.* **1998**, *37*, 2285-2290. c) M. K. Eggleston, P. E. Fanwick, A. J. Pallenberg, D. R. McMillin, *Inorg. Chem.* **1997**, *36*, 4007-4010. d) M. T. Miller, P. K. Gantzel, T. B. K. Karpishin, *J. Am. Chem. Soc*. **1999**, *121*, 4292-4293. e) C. T. Cunningham, J. J. Moore, K. L. H. Cunningham, P. E. Fanwick, D. R. McMillin, *Inorg. Chem*. **2000**, *39*, 3638-3644. f) G. Accorsi, N. Armaroli, C. Duhayon, A. Saquet, B. Delavaux-Nicot, R. Welter, O. Moudam, M. Holler, J.-F. Nierengarten, *Eur. J. Inorg. Chem*. **2010**, 164-173.

[17] A.-M. Albrecht-Gary, Z. Saad, C. O. Dietrich-Buchecker, J.-P. Sauvage, *J. Am. Chem. Soc*. **1985**, *107*, 3205-3209.

[18] L. Kohler, R. G. Hadt, D. Hayes, L. X. Chen, K. L. Mulfort, *Dalton Trans*. **2017**, *46*, 13088-13100.

[19] C. O. Dietrich-Buchecker, P. A. Marnot, J.-P. Sauvage, J. R. Kirchhoff, D. R. McMillin, *J. Chem. Soc., Chem. Commun*. **1983**, 513-515.

Entry for the Table of Contents

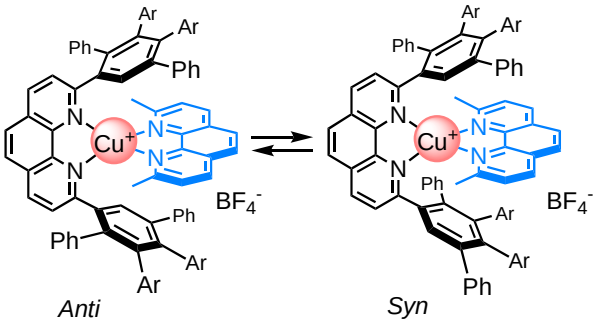

Heteroleptic bis-phenanthroline copper(I) complexes have been prepared from phenanthroline ligands substituted in their 2,9-positions with mono- and tetra-arylated phenyl groups. The resulting copper(I) complexes revealed dynamic conformational exchange between several atropisomers. Detailed NMR studies and Density Functional Theory (DFT) calculations have been carried out to assess their conformations in solution.

Institute and/or researcher Twitter usernames: @INC_CNRS - @Unistra - @LIMA_UMR7042 (Institutions) / @nierengarten6 (Researcher).